Journal of Quantitative Spectroscopy & Radiative Transfer 258 (2021) 107400

Contents lists available at ScienceDirect

Journal of Quantitative Spectroscopy & Radiative Transfer

journal homepage: www.elsevier.com/locate/jqsrt

CO_2–CO_2 and CO_2–Ar continua at millimeter wavelengths

T.A. Odintsova[a,*], E.A. Serov[a], A.A. Balashov[a], M.A. Koshelev[a], A.O. Koroleva[a], A.A. Simonova[b], M.Yu. Tretyakov[a], N.N. Filippov[c], D.N. Chistikov[d,e,f], A.A. Finenko[d,g], S.E. Lokshtanov[d,e], S.V. Petrov[d], A.A. Vigasin[e]

[a] Institute of Applied Physics of the Russian Academy of Sciences, 46 Ulyanov str., Nizhny Novgorod 603950, Russia
[b] V.E. Zuev Institute of Atmospheric Optics, Siberian Branch of the Russian Academy of Sciences, 1 Academician Zuev square, Tomsk 634055, Russia
[c] Saint Petersburg State University, Universitetskaya emb., 7/9, Saint Petersburg 199034, Russia
[d] Department of Chemistry, Lomonosov Moscow State University, GSP-1, Vorobievy Gory, Moscow 119991, Russia
[e] A.M. Obukhov Institute of Atmospheric Physics, Russian Academy of Sciences, 3 Pyzhevsky per., Moscow 119017, Russia
[f] Institute of Quantum Physics, Irkutsk National Research Technical University, 83 Lermontov str., Irkutsk 664074, Russia
[g] Center for Astrophysics | Harvard & Smithsonian, Atomic and Molecular Physics Division, 60 Garden Street, Cambridge, MA 02138, USA

ARTICLE INFO

Article history:
Received 1 September 2020
Revised 19 October 2020
Accepted 19 October 2020
Available online 20 October 2020

Keywords:
Resonator spectroscopy
Carbon dioxide
Continuum
Bimolecular absorption
Rototranslational band
Dimers
Classical trajectories

ABSTRACT

Broadband spectra of the continuum absorption in pure CO_2 gas and its mixture with Ar are studied at room temperature using a resonator spectrometer within 105–240 GHz. The expected pressure and frequency dependence is observed. The obtained data are validated by two independent calculations of the interaction-induced absorption using a semiclassical trajectory-based method. The observed continuum is interpreted in terms of bimolecular absorption, including a significant contribution from true bound dimers. A simplified formula describing both frequency and temperature dependency of the CO_2–Ar continuum within a frequency range from 60 GHz to 450 GHz at temperatures from 200 K to 400 K is suggested for use in atmospheric studies.

1. Introduction

Carbon dioxide (CO_2) is a trace gas that is known to play a crucial role in the Earth's atmosphere. Its rising amount and impact on climate change are nowadays a matter of deep concern worldwide. Being largely predominant in the present-day Venusian and Martian atmospheres [1], carbon dioxide gas determines the radiative properties of the nearest-neighbor planets. In addition, absorption by CO_2 is considered to be significant for formation and stabilization of climate regimes of some exoplanetary [2]and early planetary atmospheres [3,4]. Carbon dioxide possesses strong rovibrational line absorption in the near- and mid-infrared spectral ranges, which largely determines its role as one of the major "greenhouse gases". The spaceborne infrared sounding of the CO_2 content in the Earth's atmosphere has substantially boosted the theoretical and experimental efforts to study CO_2 resonance absorption so that accurate description of rotationally resolved CO_2 absorption is presently available within a broad spectral range (see, e.g., [5–8]). In relatively dense atmospheres, intermolecular interaction gives rise to continuum-like absorption which largely manifests itself in the troughs between dipole-permitted rovibrational bands.

Continuum absorption in pure CO_2, as well as in other pure gases, such as H_2O and N_2, was a subject of various theoretical and experimental studies during the last several decades (e.g., [9–17]and references therein). It is commonly accepted that continuum arises as a result of collisional interaction of molecules, and often collision-induced absorption (CIA) is mentioned in relation to the continuum. It is worth noting that the meaning of this term is not rigorous, and several different definitions can be found [18]. Following Ref. [19], we prefer to use the term bimolecular absorption (as a particular case of "supermolecular absorption" within the range of validity of the binary collision approximation) stressing the point that the absorption is caused by two molecules interacting with each other. Bimolecular absorption can be divided into subgroups corresponding to free molecular pairs, stable (true bound), and metastable (quasibound) dimers.

In harmony with the bimolecular origin, contributions of the different molecular pair states vary as pressure squared, although

* Corresponding author.
E-mail address: odintsova@ipfran.ru (T.A. Odintsova).

https://doi.org/10.1016/j.jqsrt.2020.107400
0022-4073/

the distinctive frequency and temperature dependencies are to be expected. It should be mentioned, however, that the definition of the continuum as the difference between the total observed and calculated resonance absorption is still quite uncertain and may also partially include the monomolecular component [20].

As for experimental works, most known studies of the continuum were devoted to water vapor due to its key contribution to the Earth's atmospheric absorption [14,21–23]. The complexity of these studies is caused by the water continuum being observed against the background of strong water resonance absorption. Thus, the magnitude of the experimentally retrieved continuum substantially depends on how precisely the resonance absorption is simulated. Moreover, the theoretical support of the water vapor continuum is still insufficient, complicating the matter of unambiguous identification of the continuum nature. Consequently, applications as yet require a well-grounded quantitative model of the water vapor continuum.

Carbon dioxide, unlike the water molecule, lacks a permanent dipole moment and, therefore, does not exhibit resonance absorption lines in the microwave and far IR range. The observed far-infrared absorption in CO_2 consists of the bimolecular component only. In a sense, the CO_2 continuum can be considered as a simplified prototype of the water vapor continuum, making it a tantalizing subject for a thorough experimental and theoretical investigation. On the one hand, unlike the water–water case there is no interference in CO_2–CO_2 between permanent and induced dipoles. This makes CO_2–CO_2 case affordable from the theoretical perspective. On the other hand, the high density of rotational energy levels in CO_2 almost prohibits nowadays the application of fully quantum methods (as in Ref. [24]) leaving virtually no feasible alternative except the use of the classical methods. The trajectory-based approach proved itself to be a practical alternative to classical many-body [17,25] perspective in the modeling of CIA band profiles. Without recourse to the adjustable parameters, good agreement with experimental spectra was demonstrated for CO_2–Ar , CO_2–Xe [11] and N_2–N_2 [15,26] molecular systems. From the standpoint of the computational cost, trajectory-based calculations are significantly cheaper than the corresponding many-body simulations.

The present study of the millimeter-wave (mm-wave) continuum in pure CO_2 and its mixture with Ar is motivated by the success of the semiclassical trajectory-based methods developed in Refs. [11,26]. The agreement, once achieved, between experimental data and calculations promotes better understanding of the nature of the continuum on a much wider scale. The continuum in CO_2 in this spectral range corresponds to its rototranslational (RT) collision-induced absorption (CIA) band. The CO_2 continuum in this spectral range is of particular interest since intermolecular vibrational bands of tightly bound dimers are expected to manifest themselves against a structureless pedestal of the CIA profile. The literature experimental data on the CO_2 continuum in the mm-wave range are scarce. Moreover, they are characterized by insufficient accuracy of measurements and were performed on a coarse frequency grid [27–39]. In this paper, we present the results of experimental and theoretical investigation of the CO_2–CO_2 and CO_2–Ar continuum absorption measured in the mm-wave range (105–240 GHz) in frequency steps of about 0.3 GHz and calculated for the whole RT band.

The paper is organized as follows. Section 2 describes the experimental approach. Section 3 deals with the experimental data analysis and continuum retrieval. The general outlines of the trajectory-based calculations performed by two independent groups are given in Section 4. Results of the experiment and calculations are compared and discussed in Section 5. Conclusions are summarized in Section 6. Experimental data on CO_2–$CO_2$and CO_2–Ar continua are given in Supplementary Materials.

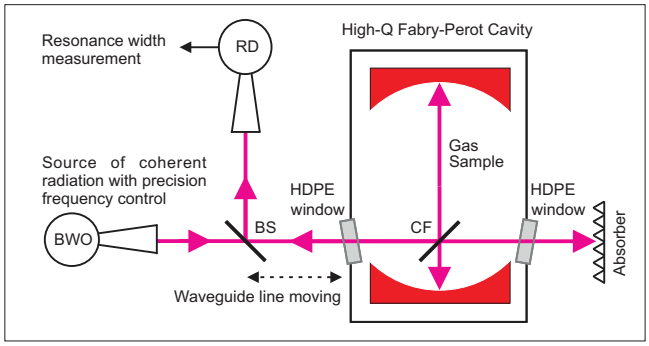

Fig. 1. Simplified diagram of the resonator spectrometer: BWO stands for Backward Wave Oscillator, RD for Radiation Detector, BS for Beam Splitter, CF for Coupling Film.

2. Experimental details

The experimental approach used in the current study is similar to the one used for measurements of the continuum absorption in nitrogen [15]. In particular, the absorption spectra were recorded using a resonator spectrometer [40], reaching a sensitivity in terms of the absorption coefficient of about 4×10^{-9} cm^{-1}. A simplified diagram of the spectrometer is presented in Fig. 1. A high-finesse (~ 3000) Fabry-Perot cavity was used as a sensing element of the spectrometer. The cavity was placed inside a vacuum chamber, which allows pressure variations from vacuum up to about 2 atm. Absorption measurements were performed at eigenfrequencies of the fundamental TEM modes of the cavity, having length L near 0.51 m and a free spectral range of about 300 MHz.

A resonance curve width of the cavity filled with non-absorbing gas (Δf_0) is defined by the cavity intrinsic losses of radiation power (reflection, coupling, diffraction). Gas absorption increases the resonance curve width (Δf) with respect to the case of absorption absence. Thus, the absorption coefficient α at frequency ν can be found from the difference of two resonance curve widths:

$$\alpha(\nu) = \frac{2\pi}{c}(\Delta f - \Delta f_0), \quad (1)$$

where c is the speed of light in vacuum.

Absorption spectra were registered in a frequency range 105–240 GHz, covered by two backward wave oscillators (BWOs) of the type of OB-76 (105–148 GHz) and OB-24 (147–240 GHz) (Istok, Fryazino, Moscow region, http://istokmw.ru). BWO frequency was stabilized by a Phase Locked Loop (PLL) against a harmonic of a microwave (8–12 GHz) synthesizer (Anritsu, MG3692C). Fast digital scanning of the BWO frequency around a chosen value without phase jumps was performed using a direct digital synthesizer PTS×10 as a reference (local) oscillator for PLL. Commercial detectors based on low-barrier planar Schottky diodes were used.

The experimental procedure was organized as follows. Firstly, the evacuated vacuum chamber was filled with a sample gas (CO_2 or mixture CO_2–Ar), and total losses of radiation power (Δf) were measured. Intrinsic cavity losses (Δf_0, the instrumental baseline) were measured at exactly the same frequencies after the chamber was evacuated and filled with non-absorbing gas (Kr or Ar) at a pressure chosen such that its refraction index is equal to that of the studied gas. Kr and Ar were chosen since their refractive indexes are close to those of CO_2 and CO_2–Ar mixture correspondingly, thus allowing minimal pressure difference between the baseline and sample spectra recordings. This minimizes the possible change of the baseline due to the changing phase of standing waves arising due to spurious reflections from chamber windows.

CO_2 and CO_2-Ar spectra were recorded at room temperature and several values of pressure ranging from 375 to 1490 Torr for

Table 1
Experimental conditions.

Sample	CO_2		CO_2–Ar	
Frequency range, GHz	105–148	147–240	105–148	147–240
Total pressure, Torr	375–1485	750–1490	903–1402	907–1406
Number of pressure points	7	4	7	7
CO_2 content, %	100		18–33	

pure CO_2 spectra and from 903 to 1406 Torr for CO_2–Ar mixture with the CO_2 mixing ratio of 18–33%. Each spectrum corresponding to a given pressure was repeated for two different positions (shifted by $\lambda/4$ along the optical axis) of the quasi-optical waveguide line relative to the cavity corresponding to the change in the phase of the standing waves by π. Averaging of such recordings notably improves the signal-to-noise ratio (SNR) of the obtained spectra (see Ref. [40] for details). Gaseous samples of CO_2 , Ar, and Kr with quoted purity of better than 99.99% were used for the experiment. Gas pressure was continuously monitored during spectra recordings by means of a pair of Baratron gauges of the ranges up to 1000 and 2000 Torr with the declared uncertainty 0.25% of reading. All spectra were recorded at 297.3 ± 1 K. Temperature was continuously measured using platinum sensors PT-100 (the uncertainty is 0.2 K) placed on edges of cavity mirrors and in free space inside the gas chamber. Temperature gradients did not exceed 0.2 K. The temperature of the elements of the quasi-optical waveguide line maintained constant during the experiment by means of an active thermostat providing high reproducibility of the spectra recordings, comparable with the spectrometer sensitivity. The experimental cycle yielded a total of fifty spectra. Table 1summarizes experimental conditions for the obtained data.

3. The continuum retrieval

Measured absorption coefficient in a gas mixture is assumed to be composed of self- (α_s) and foreign- (α_f) continuum components:

$$\alpha(\nu) = \alpha_s(\nu) + \alpha_f(\nu). \tag{2}$$

Within the binary collision approximation, each component is expected to be proportional to the product of the number densities of colliding molecules. Gas density can be calculated using partial pressures as directly measurable values and virial equation of state. At not too high pressures it is necessary to include only the second virial coefficient term. The values of the second virial coefficient for CO_2, Ar and their mixtures of [41,42] were used. The self-continuum, corresponding to the absorption coefficient of pure CO_2, was analyzed using the following equation:

$$\alpha_s(\nu) \equiv \alpha_{CO_2-CO_2}(\nu) = C_{CO_2-CO_2}(\nu) n_{CO_2}^2 = \left(\frac{\nu}{c}\right)^2 \tilde{S}_{CO_2-CO_2}(\nu) n_{CO_2}^2, \tag{3}$$

where n is a gas density in units of amagat (1 amagat $= 2.68678 \times 10^{19}$ cm^{-3}), ν is expressed in Hz, $C_{CO_2-CO_2}(\nu)$ is the continuum absorption coefficient normalized by gas density squared. We shall call the frequency-dependent function $\tilde{S}_{CO_2-CO_2}(\nu)$ the reduced spectral function. As we show below, its consideration is convenient to examine the details of the continuum absorption in the far-infrared/mm-wave range.

In a mixture with argon, the term corresponding to pure argon continuum vanishes because the dipole of a pair of identical atoms equals zero. Consequently, no induced absorption can be observed in pure argon, which is proportional to the argon density squared. This statement is valid, however, provided the gas density is low enough not to step beyond the binary collisions approximation [19]. In our case, a very weak continuum caused by triple collisions, if any, is excluded with the baseline subtraction. The foreign-continuum was considered as

$$\alpha_f(\nu) \equiv \alpha_{CO_2-Ar}(\nu) = C_{CO_2-Ar}(\nu) n_{CO_2} n_{Ar} = \left(\frac{\nu}{c}\right)^2 \tilde{S}_{CO_2-Ar}(\nu) n_{CO_2} n_{Ar}. \tag{4}$$

The ν^2-factor was introduced in Eqs. (3), (4) because of the following considerations. In the long-wave part of the spectrum, including the mm-wave range, the frequency dependence of the continuum is mainly determined by the radiation term (see, e.g., [19]). In this range, the condition $h\nu \ll k_B T$ is satisfied, and the radiation term has predominantly frequency-squared dependence. Therefore the reduced spectral function $\tilde{S}(\nu)$ converges to the ordinary spectral function $S(\nu)$, up to a constant factor, in the long-wave limit.

Binary absorption coefficient $C(\nu)$ can be obtained from the spectral function $S(\nu)$ using

$$C(\nu) = \frac{(2\pi)^4 V}{3\,hc} \nu \left[1 - \exp\left(-\frac{h\nu}{k_B T}\right)\right] S(\nu), \tag{5}$$

where k_B and h are Boltzmann and Plank constants, respectively. T and V refer to the gas temperature and volume.

Empirically determined foreign- and self-continuum absorption coefficients are usually fitted to the frequency-squared dependence (e.g., N_2 [15], dry air [43], and H_2O [44–46])

$$C(\nu) = k\nu^2, \tag{6}$$

where k is a frequency-independent parameter. This approximation implies that spectral functions of molecular pairs have to be constant within the whole frequency range in question. Our experimental and theoretical analysis, the results of which are reported below, proves, however, that this is not true. Instead of a constant parameter k we shall consider hereafter the reduced functions $\tilde{S}(\nu)$ defined by relevant expressions (3) and (4).

Fig. 2 shows the totality of our measured experimental points, which are represented in terms of $C_{CO_2-CO_2}(\nu)$ and $C_{CO_2-Ar}(\nu)$ continua, i.e., in terms of respective absorption coefficients $\alpha(\nu)$properly normalized by the CO_2 density squared or by the product of CO_2 and Ar densities. Good agreement of the continuum absorption recorded using two different BWOs in two partially overlapping frequency ranges (105–148 and 147–240 GHz) is prominent. It serves as a consistency test of the obtained data. Good agreement of $C_{CO_2-CO_2}(\nu)$ retrieved from the spectra obtained at different CO_2 pressures confirms the expected quadratic pressure dependence and allows collected data at every frequency point to be averaged, thus leading to a significant reduction of the noise (by a factor of two in terms of the standard deviation).

Following Eqs. (2)–(4), the foreign-continuum $\alpha_{CO_2-Ar}(\nu)$ was determined as a difference between the measured absorption in the CO_2–Ar mixture and corresponding self-continuum $\alpha_{CO_2-CO_2}(\nu)$. The magnitude of the retrieved foreign-continuum, and thus, the SNR, is approximately 3–4 times lower than for the self-continuum. Consistency of the data obtained at different pressures and frequency ranges within the experimental uncertainty can be stated. Averaging of spectra recorded at different pressures yield an improvement of the SNR by a factor of two.

Table 2
Fitted parameters in Eq. (7) at $T = 297.3$ K.

	CO_2–CO_2	CO_2–Ar		
	experiment	experiment	theory IAP/MSU	theory SPbSU
$A_0, 10^{-8}$ cm amagat^{-2}	6.11	2.09	1.945	2.153
$B_0, 10^{-7}$ GHz^{-2}	0	2.778	2.778	5.502
$C_0, 10^{-9}$ cm amagat^{-2}	2.43	7.02	7.885	9.055
D_0, GHz	0	98.56	98.56	100.2
E_0, GHz	306.8	68.75	57.62	59.00

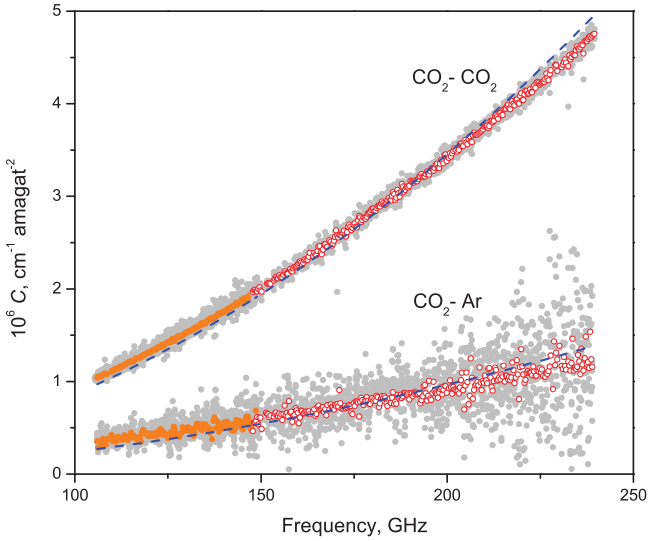

Fig. 2. Frequency variation of CO_2–Ar and CO_2–CO_2 binary absorption coefficients withinspectral ranges 105–149 GHz (orange) and 147–240 GHz (red) retrieved from the series of measurements at total pressures varying from 375 to 1490 Torr (grey) at 297.3 K; approximation of experimental data with frequency squared function (dashed curves). Consistency between obtained spectra corresponding to different experimental conditions is demonstrated. (For interpretation of the references to color in this figure legend, the reader is referred to the web version of this article.)

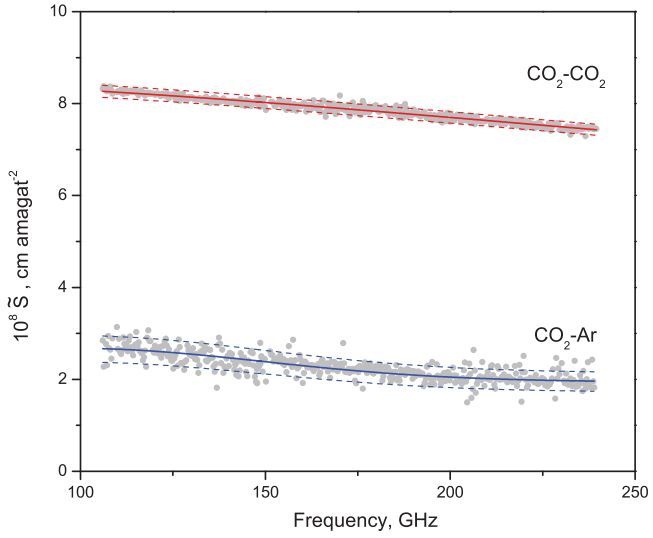

Fig. 3. Reduced spectral functions: experimental data of $\tilde{S}_{CO_2-CO_2}(\nu)$ (upper grey dots) and $\tilde{S}_{CO_2-Ar}(\nu)$ (bottom grey dots); approximations of $\tilde{S}_{CO_2-CO_2}(\nu)$ (red solid) and $\tilde{S}_{CO_2-Ar}(\nu)$ (blue solid), overall uncertainty (dashed curves). (For interpretation of the references to color in this figure legend, the reader is referred to the web version of this article.)

The dashed lines in Fig. 2 show the fit of Eq. (6) to the experimental data. It is seen from Fig. 2 that the parabolic shape of the frequency dependence imposed by Eq. (6) is insufficient to accurately represent experimental data within the entire spectral range.

For the sake of upcoming applications we suggest approximation for the $\tilde{S}_{CO_2-Ar}(\nu)$ spectral function by the following expression:

$$\tilde{S}(\nu) = A_0\left(1 - B_0\nu^2\right) + C_0 \exp\left(-\frac{(\nu - D_0)^2}{E_0^2}\right), \qquad (7)$$

where A_0, B_0, C_0, D_0, E_0 are parameters relevant to the temperature of the experiment, *i.e.* 297.3 K.

The values of parameters obtained through nonlinear least-squares fit of the function to the experimental and theoretical data are collected in Table 2.

Trajectory-based calculations were performed independently by the Saint Petersburg State University (SPbSU) and the Obukhov Institute of Atmospheric Physics/Lomonosov Moscow State University (IAP/MSU) groups. The above acronyms are used hereafter throughout this paper. It should be noted that although Eq. (7) can be fitted to the $\tilde{S}_{CO_2-CO_2}$ reduced spectral function, the resulting parameters are not comparable to those obtained for CO_2–Ar. Nevertheless, the fit of the experimental data is useful for subsequent analysis of the CO_2–Ar data. The relevant parameters are shown in Table 2; in the fitting procedure of the CO_2–CO_2 data, the parameters B_0 and D_0 were fixed at zero values. Experimental data on reduced spectral functions $\tilde{S}_{CO_2-CO_2}(\nu)$ and $\tilde{S}_{CO_2-Ar}(\nu)$ together with their approximations are presented in Fig. 3.

Table 3
Uncertainty budget (in terms of relative percentage, corresponding to one standard deviation).

Relative contribution	$\tilde{S}_{CO_2-CO_2}(\nu)$	$\tilde{S}_{CO_2-Ar}(\nu)$
Statistical uncertainty	0.8	8.5
Gas sample temperature	0.95	0.8
Number density	0.86	1
Mirror temperature	0.1	0.1
Water vapor	0.4	5.5
Uncertainty of $\tilde{S}_{CO_2-CO_2}(\nu)$	–	1.6
Overall uncertainty	1.6	10.3

We evaluated the uncertainty of the obtained spectral functions as composed of statistical uncertainty related to experimental noise, the uncertainty of pressure and temperature measurements, and the absorption uncertainty related to water vapor ever-present in the gas sample and/or in the spectrometer chamber as an impurity. Table 3 summarizes the complete uncertainty budget.

The statistical uncertainty was evaluated as 1σ (standard deviation) of experimental points from a smooth approximating function Eq. (7). For $\tilde{S}_{CO_2-CO_2}(\nu)$ and $\tilde{S}_{CO_2-Ar}(\nu)$ it constitutes less than 0.8% and 8.5%, respectively. Uncertainty of the retrieved spectral functions related to gas temperature instability can be estimated using theoretically calculated temperature dependence. We used data reported in Section 4 for CO_2–Ar and preliminary results of similar trajectory-based calculations for CO_2–CO_2at 290–310 K [47]. The corresponding uncertainties are 0.95% and 0.8% for

CO_2-CO_2 and CO_2–Ar, respectively. Combined uncertainty of the molecular number density, originating from uncertainty of pressure (0.25%) and temperature (0.33%) measurements, leads to uncertainty of 0.86% and 1% for $\tilde{S}_{CO_2-CO_2}(\nu)$ and $\tilde{S}_{CO_2-Ar}(\nu)$, respectively.

It should be mentioned that the temperature of resonator mirrors affects their reflectivity, which in turn influences the instrumental baseline. Therefore, its variation may cause overestimation or underestimation of the observed continuum absorption. The temperature of both mirrors was continuously measured during the experiment, and its variations were taken into account using the known temperature dependence of the reflectivity of the mirrors [48]. Note that this correction was negligible (less than 0.3%) for all spectra. Uncertainty of the retrieved spectral functions related to this correction is mostly due to the mirror temperature measurement error (0.2 K) and is less than 0.1% for both functions.

The presence of water vapor as a minor impurity in the studied gas results in additional absorption caused by H_2O-CO_2 and H_2O-Ar pairs and thus may lead to overestimation of observed CO_2 and CO_2-Ar continua. The water vapor line near 183 GHz with an integrated intensity of 7.785×10^{-23} cm/molec at 296 K was not observed in the pure CO_2 spectra. The maximum possible partial pressure of water vapor in the CO_2 sample was evaluated as less than 5 mTorr from the assumption that the absorption at the line maximum is smaller than one standard deviation of the experimental noise. The corresponding potential contribution of H_2O-CO_2 continuum to the observed absorption was estimated using data from Table 2 of Ref. [28], where the experimentally determined absorption coefficient of the H_2O-CO_2 mixture at 239.37 GHz is presented. (Note that the contribution of water monomer absorption resulting from neighboring resonance lines is negligible at this frequency under conditions of the experiment.) The contribution of the H_2O-CO_2 continuum was estimated using Eq. (6), supposing that the continuum follows quadratic frequency dependence. The related uncertainty of the CO_2-CO_2 spectral function was found to be less than 0.4%.

In the case of the CO_2-Ar mixture, the 183-GHz water line was not seen in the single spectrum recording, but its manifestation appeared after averaging of all recorded spectra. Corresponding water vapor partial pressure was evaluated to be about 15 ± 2 mTorr. Related water vapor monomer absorption was calculated and subtracted from the averaged spectrum. Contributions of H_2O-Ar and H_2O-CO_2continua were calculated using Eq.(6) and related experimental data at 239.37 GHz of Refs. [49] and [28], respectively. The former is found to be negligible, while the latter amounts to less than 5.5% under considered conditions.

The overall uncertainty of the obtained spectral functions was found as the square root of the sum of all aforementioned uncertainties squared. For CO_2-CO_2 it amounted to 1.6%. Uncertainty of $\tilde{S}_{CO_2-Ar}$includes uncertainty of $\tilde{S}_{CO_2-CO_2}$, as it follows from Eqs. (2)–(4). The overall uncertainty of the CO_2–Ar spectral function adds up to 10.3%.

4. Classical trajectory-based simulation of the CIA rototranslational spectra

In recent years the tendency in the simulation of the CIA spectra concentrates more and more on the methods which are free from the use of adjustable parameters. This concerns both the development of the new formalisms aimed at simulation of the CIA spectral profiles with no recourse to empirical corrections and the use of quantum-chemical *ab initio* methods to characterize pairwise intermolecular interaction. Whilst the use of the *ab initio* calculated potential energy surface (PES) has become almost a routine, the interaction induced dipole surface (IDS) is often represented as a sum of the main electrostatic terms, *i.e.*, with no resort to more accurate quantum-mechanical consideration. On the one hand, the use of a simplified IDS is advantageous because it permits one to circumvent a portion of heavy quantum-chemical calculations. On the other hand, pure *ab initio* calculated IDS is certainly more precise at least at close intermolecular separations, which can be reached, *e.g.*, during collisions at elevated temperature [50].

Impressive results in theoretical CIA spectroscopy have been achieved in recent years using pure quantum mechanical [16], molecular dynamics [17,25], and quasiclassical trajectory-based simulation [11,26,51]. In this section, we report the results of the trajectory-based investigations, which were carried out independently by SPbSU and IAP/MSU research groups . In the pioneering paper [11] by the SPbSU group, the induced CO_2–Ar RT CIA band was considered including the contribution from true bound dimers. Whilst calculating the IDS, only the principal electrostatic terms were taken into account. Later on, analogous research was undertaken by the IAP/MSU group using complete *ab initio* PES and IDS [52]. A brief overview of the relevant methods and obtained results are given, respectively, in the subsections below.

4.1. SPbSU trajectory based simulation of CO_2–Ar CIA RT band with ab initio PES and simplified IDS

In the mm-wave range, the classical spectral function $S^{cl}(\nu)$ can be written as

$$S^{cl}(\nu) = \frac{1}{2\pi}\int_{-\infty}^{+\infty} \Phi(t) e^{-2\pi i \nu t} dt, \tag{8}$$

where $\Phi(t)$ is the autocorrelation function of the interaction induced dipole.

In the calculations of the autocorrelation function, we use the method of classical 3D trajectories based on classical dynamics of both the translational motion of colliding particles and the rotation of the absorbing molecule. The classical consideration of rotation, in this case, should not lead to significant contour distortions since the CIA bands (with the exception of the spectra of the hydrogen molecule) should have a smooth broad shape without resolved rotational structure. The classical trajectory method used in this section was described in detail in Ref. [11].

Step-by-step changes in the orientation of the molecule and the relative position of the particles are calculated in the laboratory reference frame. This method allows us to distinguish the spectral contributions of true bound states, free pairs states trajectories, and trajectories with the formation of metastable dimers. The contribution of true dimers and other contributions were calculated using two different algorithms described in Ref. [11]. In calculating the spectral function, we limited the multipole expansion to the most important contribution to the induced dipole of CO_2–Ar pairs, which is the polarization of the atom in the electric multipolar (quadrupolar and hexadecapolar) field of the molecule. In describing the CO_2–Ar interaction, we used the split repulsion PESfollowing Hutson et al. [53]. The results of such calculations closely agree with those obtained with the updated PES [54].

The integrated intensities of the resulting classical spectral function (zeroth spectral moment M_0) were compared with that calculated using the phase space integral using Eq. (17). There is a slight difference of about 4% between the values calculated by the foregoing methods (see Table 1 from [11]). When comparing the calculated bandshapes with the experiment, we used the values of M_0 derived as phase space averages instead of simulated ones.

The classical spectral function $S^{cl}(\nu)$ cannot be used instead of $S(\nu)$ in the formula (5). For the quantum mechanical spectral function $S(\nu)$, the detailed balance relation must be fulfilled

$$S(-\nu) = S(\nu)\exp\left(-\frac{h\nu}{k_B T}\right), \tag{9}$$

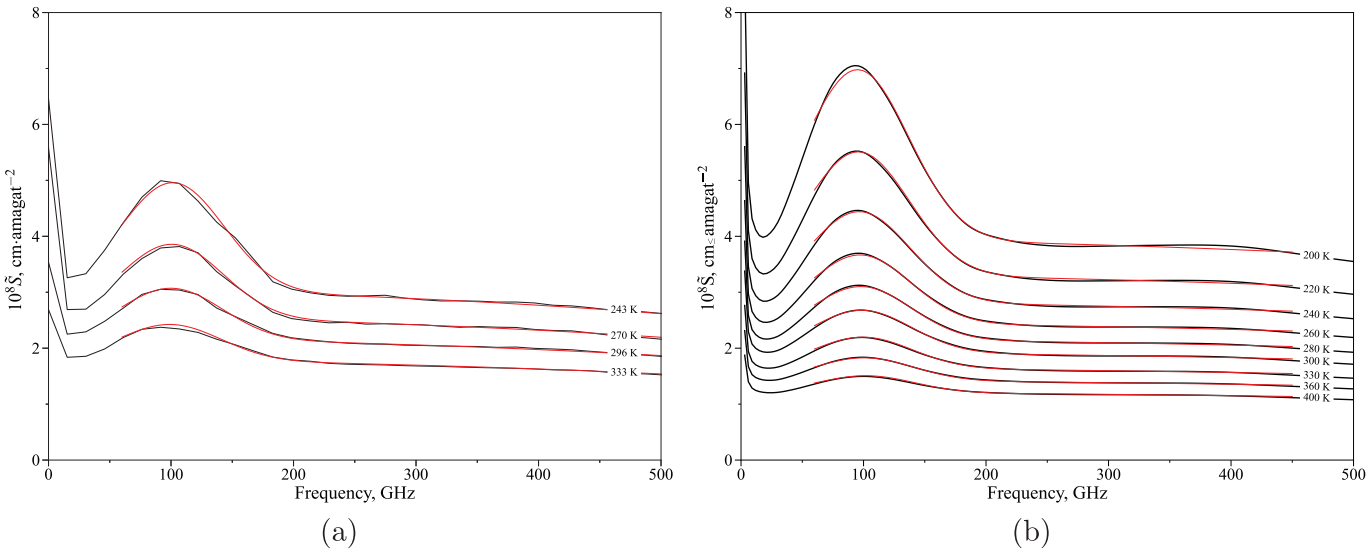

Fig. 4. Calculated CO_2–Ar reduced spectral function (black lines) issued from SPbSU (a) and IAP/MSU (b) groups at temperatures, respectively, from 243 to 333 K and from 200 to 400 K. The fits by expression (7) are shown in red. (For interpretation of the references to color in this figure legend, the reader is referred to the web version of this article.)

whereas the classical spectral function $S^{\mathrm{cl}}(\nu)$ is symmetric

$$S^{\mathrm{cl}}(-\nu) = S^{\mathrm{cl}}(\nu). \tag{10}$$

It permits one to put it in line with a symmetrized quantum mechanical spectral function

$$S^{\mathrm{sym}}(\nu) = \frac{1}{2}[S(\nu) + S(-\nu)] = \frac{1}{2}\left[1 + \exp\left(-\frac{h\nu}{k_B T}\right)\right] S(\nu) \tag{11}$$

whence follows

$$S(\nu) = 2\left[1 + \exp\left(-\frac{h\nu}{k_B T}\right)\right]^{-1} S^{\mathrm{cl}}(\nu). \tag{12}$$

Using Eqs. (4), (5) and (12), we calculated the values of $C_{CO_2-Ar}(\nu)$ and $\tilde{S}_{CO_2-Ar}(\nu)$ in the temperature range from 243 to 333 K. In the spectral interval from 60 to 500 GHz, Eq. (7) was fitted to a set of trajectory-based reduced spectral functions through the standard nonlinear least-squares routine. The subsequent fit of obtained parameters entering Eq. (7) to polynomial functions was performed to characterize the temperature dependence. A set of polynomials with degrees $(n_A, n_B, n_C, n_D, n_E) = (2, 0, 2, 1, 0)$was sufficient to closely reproduce calculated data in the specified temperature range

$$X(T) = \sum_{k=0}^{n_X} X_k (T - T_0)^k, \tag{13}$$

where $X = A, B, C, D, E$ and $T_0 = 297.3$ K.

The reduced spectral function $\tilde{S}(\nu, T)$ at temperature T can be reconstructed using parameters of Table 2 and Table 4 and the following equation

$$\tilde{S}(\nu, T) = A(T)(1 - B(T)\nu^2) + C(T)\exp\left(-\frac{(\nu - D(T))^2}{E(T)^2}\right). \tag{14}$$

The calculated and adjusted reduced spectral functions are shown in the Fig. 4(a). The values of the fitting parameters are given in Table 4.

Table 4
Fitted parameters in Eq. (13).

Parameters	SPbSU	IAP/MSU
$A_1, 10^{-10}$ cm amagat $^{-2}$ K^{-1}	−1.267	−1.084
$A_2, 10^{-13}$ cm amagat $^{-2}$ K^{-2}	6.776	5.385
$A_3, 10^{-15}$ cm amagat $^{-2}$ K^{-3}	–	−3.269
$A_4, 10^{-17}$ cm amagat $^{-2}$ K^{-4}	–	1.428
$C_1, 10^{-11}$ cm amagat $^{-2}$ K^{-1}	−11.96	−8.440
$C_2, 10^{-13}$ cm amagat $^{-2}$ K^{-2}	13.35	6.384
$C_3, 10^{-15}$ cm amagat $^{-2}$ K^{-3}	–	−5.951
$C_4, 10^{-17}$ cm amagat $^{-2}$ K^{-4}	–	3.204
$D_1, 10^{-2}$ GHz K^{-1}	−2.648	3.447
$E_1, 10^{-2}$ GHz K^{-1}	–	−1.569

4.2. IAP/MSU simulation of CO_2–Ar and CO_2–CO_2 CIA RT bands using complete ab initio PES and IDS

The salient features of our trajectory-based approach concerning the simulation of RT CIA spectra in N_2–N_2, CO_2–Ar, and CO_2–CO_2 are reported elsewhere [15,26,52]. The *ab initio* calculated values on a discrete grid of sampling points are subject to multidimensional fitting, in which properly chosen radial dependencies of the energy and the dipole moment are complemented by the angular expansions in a Legendre series. Four principal novelties in our trajectory-based simulation of the RT CIA spectra are worth mentioning here, which mark a distinction of the present method from that reported by us previously in Ref. [26]. First, we consider the trajectory dynamics problem in a laboratory-fixed reference frame instead of the body-fixed one. The main impetus for this change consists in our intention to mitigate the problem of singularity in a dynamical problem solution, the nature of which was described in Ref. [26]. Note that singularities are still present in the system of dynamical equations relevant to the laboratory-fixed frame. However, the integration of the dynamical equations in the neighborhood of singularities is managed more robustly by numerical methods in the case of the laboratory-fixed frame rather than that of body-fixed. Thus trajectory propagation in a laboratory-fixed frame can be efficiently performed without recourse to the technique of relocating the singularities in the phase space based on the canonical variable change [26]. Second, in this work, the contribution to absorption from true bound dimers,

which was previously disregarded in Refs. [15,26], is taken into account. Third, the initial conditions for the massive trajectory simulation are generated using the Boltzmann-weighted distribution of canonical variables. The identical procedure is adopted for both free/quasi-bound and true bound molecular pairs. The details of this innovative computational scheme can be found in a separate paper [52]. It is worth mentioning that, given the purely classical spectral function is obtained, there exists no rigorous procedure to make it satisfy the quantum principle of detailed balance (9). Several approximate procedures were suggested in the literature [19], of which the formula (12) is an example. In the present section, we use a somewhat different desymmetrization procedure:

$$S(\nu) = \exp\left(\frac{h\nu}{2k_B T}\right) S^{\mathrm{cl}}(\nu). \tag{15}$$

Interestingly, the desymmetrization procedures (12) and (15) give nearly identical spectral profiles over the whole RT band. Lastly, a procedure for reweighing of the trajectory ensemble was implemented, allowing for obtaining multiple CIA spectra within a reasonable temperature range [52].

Employing our multitemperature reweighing procedure, we performed calculations of CO_2–Ar RT CIA spectra from 200 K to 400 K with 10 K step (with several additional temperatures included at about room temperature). We opted to perform trajectory-based calculations of free/quasibound and true bound states independently to thoroughly monitor the convergence of respective spectral profiles with respect to the number of trajectories. It was found out that 1 and 20 million trajectories for true bound and free/quasibound pair states, respectively, is sufficient to achieve reasonable convergence over the entire range of RT CIA profile in the studied temperature range. Although a significantly smaller number of trajectories is required to ensure convergence over the true bound states region of phase space, the simulation is drastically more time-consuming than that of free states. In the spectral interval from 60 to 450 GHz, the Eq. (7) was fitted to a set of trajectory-based reduced spectral functions. Due to a broader temperature range, polynomials of higher degrees were required to characterize the temperature dependence of parameters in Eq. (13). We opted to use polynomials of degrees $(n_A, n_B, n_C, n_D, n_E) = (4, 0, 4, 1, 1)$ for sufficient representation of our data.

The trajectory-based calculation of the CO_2–CO_2 RT CIA was performed at 297 K. Same as for CO_2–Ar , 20 million trajectories for the free/quasibound pair states were found to be sufficient for a reasonable convergence, whereas 300 thousand trajectories properly sample the region of phase space pertaining to bound states.

We control the accuracy of our trajectory-based calculations by comparison of two low-order spectral moments, which can be found either by the integration of the band shape over frequency domain

$$M_n{}^{spec} = V \int_{-\infty}^{+\infty} \nu^n S^{\mathrm{cl}}(\nu) \mathrm{d}\nu, \quad n = 0, 2, \tag{16}$$

or by the integration of the Boltzmann-weighted squared dipole moment function $\boldsymbol{\mu}$ and square of its time derivative $\dot{\boldsymbol{\mu}}$ over the phase space

$$M_0{}^{phas} = \frac{V}{4\pi\varepsilon_0} \frac{1}{2\pi c} \langle \boldsymbol{\mu}^2 \rangle, \tag{17}$$

$$M_2{}^{phas} = \frac{V}{4\pi\varepsilon_0} \frac{1}{(2\pi c)^2} \langle \dot{\boldsymbol{\mu}}^2 \rangle. \tag{18}$$

Here ε_0 is the vacuum permittivity, and angular brackets denote Boltzmann averaging. The details of how the low-order spectral moments are calculated can be found in Ref. [52]. Table 5 contains calculated values of the zeroth and second spectral moments corresponding to the free/quasi-bound (*i.e.*, unbound states having total energy in excess of dissociation threshold) and true bound dimer portions of the phase space. By true bound dimers we consider those whose total Hamiltonian is less than zero ($H < 0$).

Table 5
Zeroth (in cm^{-1} $amagat^{-2}$) and second (in cm^{-3} $amagat^{-2}$) spectral moments for RT band of CO_2–Ar and CO_2–CO_2 at T = 297 K. Superscripts (spec) and (phas) mean, respectively, the values derived from either the frequency domain using Eq. (16) or the phase space integration using Eqs. (17) and (18).

	CO_2–Ar		CO_2–CO_2	
	unbound	true bound	unbound	true bound
M_0^{spec}	0.00036526	0.000015958	0.00105699	0.00010804
M_0^{phas}	0.00036503	0.000016085	0.00105495	0.00010841
M_2^{spec}	0.63678642	0.00441571	1.90326747	0.06141518
M_2^{phas}	0.63140654	0.00444949	1.89296660	0.06193392

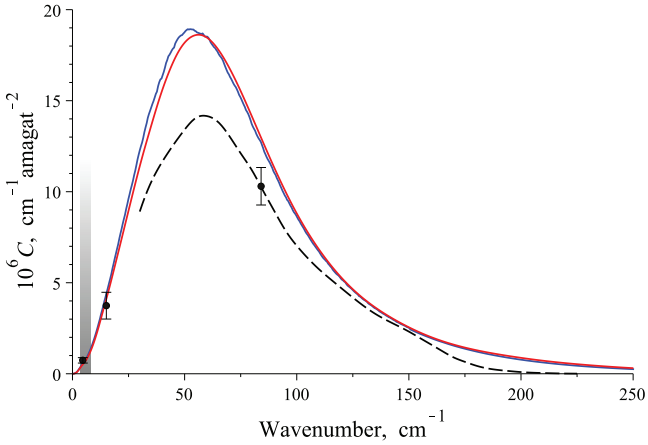

Fig. 5. CO_2–Ar binary absorption coefficient. Trajectory-based (IAP/MSU $T = 298$ K in red, SPbSU at $T = 296$ K in blue, solid lines) and experimental ([55], FIR spectrometer data and FIR laser data at $T = 298$ K are represented with dashed line and solid points, respectively) spectra. The shaded area shows the spectral range of our experiment. (For interpretation of the references to color in this figure legend, the reader is referred to the web version of this article.)

It is seen that the difference between both moments as calculated independently varies from 0.06% to 0.8%. This good agreement can be considered as a clear indication of the reliability of our calculated trajectory-based spectra because their major integrated characteristics are perfectly compatible with their relevant statistically weighted counterparts.

5. Discussion

A comparison of absorption in CO_2–Ar CIA RT band at $T = 298$ K calculated by SPbSU and IAP/MSU groups and experimental data is shown in Figs. 5 and 6. Fig. 5 demonstrates a good agreement of SPbSU and IAP/MSU calculation results within the entire range of the CIA RT band (the normalized root-mean-square deviation doesn't exceed 5% for the spectral range up to 250 cm^{-1}). The agreement of the calculated and FIR experimental data [55] can be classified only as qualitative. It is notable both in the vicinity of the band maximum and in the high frequency wing. The experimental uncertainty stated by authors in Ref. [55] amounts for selected measurements to roughly 18%, but even larger deviation can be expected, as can be seen in Fig. 5, e.g., in the spectral range above ~150 cm^{-1} . The comparison with much more precise room-temperature mm-wave range data is shown in Fig. 6.

Evidently, the result of our trajectory-based simulation is in excellent agreement with reported experimental data. Moreover, the obtained CO_2–Ar reduced spectral function is in a reasonable agreement with until recently the only available four measured

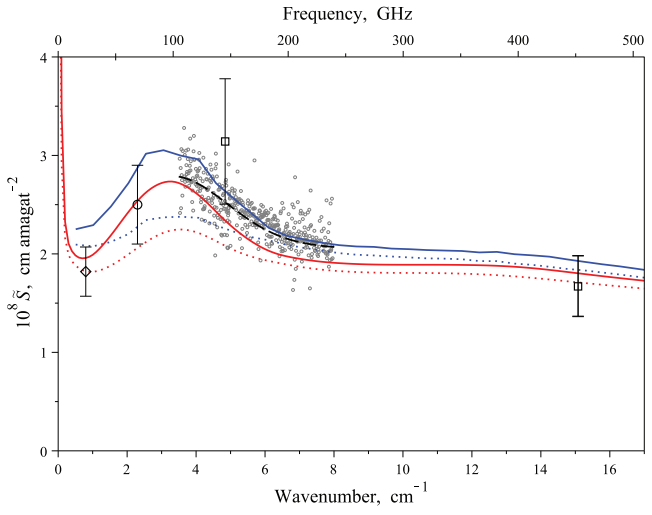

Fig. 6. Reduced spectral function for CO_2–Ar . Trajectory-based results issued from IAP/MSU (at $T = 297.3$ K) and SPbSU (at $T = 296$ K) groups are shown in red and blue, respectively. Solid lines relate to $\tilde{S}(\nu)$ obtained for complete phase space, whereas dotted line show $\tilde{S}(\nu)$ obtained provided the contribution from true bound states is ignored. Our experimental measurements at $T = 297.3$ K are given by gray circles, and dashed line is the fit of Eq. (7) to the data. The previous experimental measurements are shown by the following symbols: ○ [29],□[55],◇[56]. (For interpretation of the references to color in this figure legend, the reader is referred to the web version of this article.)

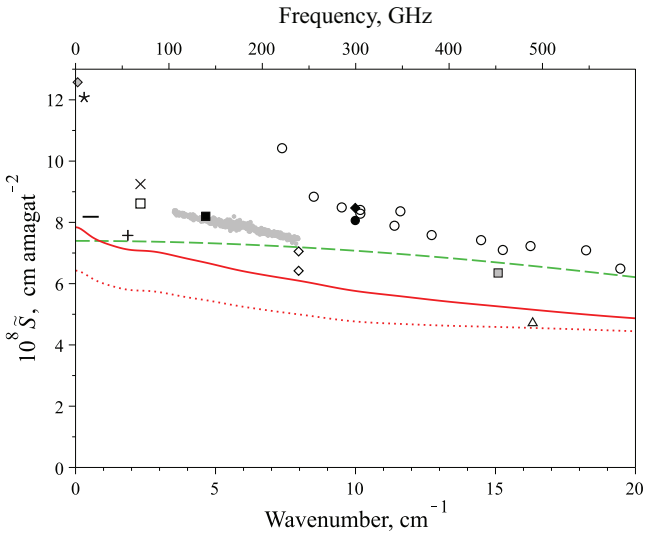

Fig. 7. Calculated and experimental reduced spectral functions for CO_2–CO_2 at $T = 297$ K. Solid line relates to IAP/MSU calculations carried out for complete phase space, whereas dotted line shows $\tilde{S}(\nu)$ provided the contribution from true bound states is ignored. Dashed line represents Gruszka and Borysow [17] calculated results (issued from the program [61] described in their paper). The experimental measurements are shown with following symbols: ● [This work], ○ [27],◇[28],×[29],●[30],□[31],△[32],■[33],+[34],⋆[35],- [36],□[37],◆[38],◇[39].

points [29,55,56] in the far-infrared/microwave spectral range. In the spectral range from 100 GHz to 240 GHz, the mean normalized root-mean-square deviation of the reduced spectral function calculated by IAP/MSU and SPbSU groups from the averaged experimental data reported in this work does not exceed 2.2% and 2.5%, respectively.

Interestingly, the contribution from true bound CO_2–Ar dimers is by no means negligible within this narrow spectral range because this frequency interval is close to the maximum of the *R*-branch of the pure rotational CO_2–Ar dimer band. The contribution from true bound CO_2–Ar dimers to the whole RT binary absorption profile is expectedly almost negligible for CO_2–Ar at near room temperature. In contrast, it is not the case for CO_2–CO_2. It is seen from Table 5 that the contribution of true bound CO_2–CO_2 dimers into the calculated zeroth spectral moment amounts to about 9%. This value is in excellent agreement with the previous estimate based on analysis of CIA in the Fermi dyad and triad spectral ranges [57] as well as on the early theoretical predictions [58,59].

The comparison of our trajectory-based CO_2–CO_2 reduced spectral function with available experimental data, including those measured in this work is shown in Fig. 7. It should be mentioned that the uncertainty of our experimental data (1.6%) is substantially smaller than that of previous measurements in this frequency range [27,28,33]. The uncertainty of measurements performed in Refs. [27] and [33] amounts to 10% and 2.3%, respectively. The uncertainty of measurements in Ref. [28] was not evaluated by authors, however, the discrepancy between two provided points corresponding to the same thermodynamic conditions is 9%. The agreement of our results with data of Refs. [28,33] within experimental uncertainty is observed. The relative difference between our data and data of Ref. [27] exceeds 20%, which is almost twice as much as the joint experimental uncertainty. Also shown is the result of molecular dynamics simulation from Gruszka and Borysow [17], which, in terms of the binary absorption coefficient, is adapted in the recent update of the relevant section of the HITRAN database [60]. The notable distinction between our calculated results and those from [17] can be referred, in particular, to improper taking into account the contribution from true bound dimers in Ref. [17]. Note that the integrated bandshape intensity in Ref. [17] was adjusted to experimental data of Ho et al. [27] by introducing the parametrized overlap corrections to the expansion of induced dipole.

The IAP/MSU curve in Fig. 7 shows a rate of spectral function decrease coinciding almost ideally with what was observed in our experiment, although the absolute values are regularly lower than our experimental ones by about 20%.

We can tentatively suggest that the reason for such a non-negligible deviation results from our assumption of the rigidity of CO_2 molecule. In reality, even at near room temperature, the low-lying CO_2 bending mode is excited so that nearly 7.6% of monomers are in their (010) excited state. This small fraction of excited molecules may have a strong impact on intermolecular induction because the dipole associated with the bent vibrationally excited molecule is apt to effectively induce the dipole in the neighboring linear CO_2 molecule in its ground state. To take this effect into account a new set of calculations is worth doing, having lifted the above-mentioned assumption, *i.e.*, presupposing unfrozen vibrations in a CO_2 molecule.

6. Conclusions

Continua absorption in pure CO_2gas and in its mixture with Ar are measured at room temperature and pressures up to 2 atm (375–1490 Torr) over a broad spectral range (105–240 GHz) using resonator spectrometer. The expected pressure dependence of the continua is verified. The frequency variation of the mm-wave continua absorption is shown to deviate significantly from quadratic behavior. The relevant spectral function is parameterized based on both experimental data at room temperature and theoretical values obtained for the broad temperature range. In-depth semiclassical trajectory-based analysis of CIA in the long-wave spectral range of CO_2–X (X = Ar or CO_2) is undertaken by two independent research groups. The result of this analysis is compared with the obtained experimental data. Excellent agreement of measured and calculated CO_2-Ar continuum

is demonstrated validating both experimental and theoretical approaches. Since no data for RT CIA of the CO_2−Ar system is currently available in the HITRAN database, we propose the addition of trajectory-based results reported in this work to the relevant section of the database. As far as CO_2–CO_2continuum is concerned, a good qualitative and reasonable quantitative agreement is achieved.

Despite the use of somewhat different theoretical approaches, both SPbSU and IAP/MSU groups concluded that the trajectory-based method has an excellent perspective for widespread adoption in the interests of CIA spectral simulation. The reasons for that conclusion are the feasibility from the computational standpoint and reasonable accuracy at least when the interaction with light molecules, *e.g.*, hydrogen, is excluded from consideration. A comparison of theoretical results obtained by both groups allows us to draw some useful conclusions. First, the use of either complete *ab initio* dipole surface by the IAP/MSU group or a simplified IDS by SPbSU group results in nearly perfect agreement with current microwave experimental results and suffices to obtain good agreement within the whole spectral range of absorption profile . Second, the use of different desymmetrization procedures doesn't cause a perceptible difference in the calculated CO_2–Ar spectral profiles, at least at 297 K and within the spectral range in question. Lastly, the simulation of absorption by true bound states requires substantially more computational power than that of free states.

Declaration of Competing Interest

The authors declare that they have no known competing financial interests or personal relationships that could have appeared to influence the work reported in this paper.

CRediT authorship contribution statement

T.A. Odintsova: Investigation, Data curation, Writing - original draft. **E.A. Serov:** Investigation, Methodology. **A.A. Balashov:** Investigation. **M.A. Koshelev:** Validation, Methodology. **A.O. Koroleva:** Investigation. **A.A. Simonova:** Investigation. **M.Yu. Tretyakov:** Conceptualization, Methodology, Writing - review & editing. **N.N. Filippov:** Methodology, Writing - original draft. **D.N. Chistikov:** Methodology, Software, Writing - original draft. **A.A. Finenko:** Methodology, Software, Writing - original draft. **S.E. Lokshtanov:** Methodology, Software, Writing - original draft. **S.V. Petrov:** Methodology. **A.A. Vigasin:** Conceptualization, Writing - original draft, Writing - review & editing, Supervision.

Acknowledgments

The experimental studies and data analysis were supported by the Russian Foundation for Basic Research, Grants 18-32-20156, and 18-05-00119. Partial support of this work from The Ministry of Science and Higher Education of the Russian Federation, Project 19-270, and from Presidium of RAS Program 12 is gratefully acknowledged. The trajectory-based calculations of the IAP/MSU group were run on the FASRC Cannon cluster supported by the FAS Division of Science Research Computing Group at Harvard University.

Supplementary material

Supplementary materials contain experimental data on CO_2–$CO_2$and CO_2–Ar continua. Supplementary material associated with this article can be found, in the online version, at doi:10.1016/j.jqsrt.2020.107400.

References

[1] Bézard B, Fedorova A, Bertaux JL, Rodin A, Korablev O. The 1.10-and 1.18-μ.nightside windows of Venus observed by SPICAV-IR aboard Venus Express. Icarus 2011;216(1):173–83.
[2] Levi A, Sasselov D, Podolak M. The abundance of atmospheric CO_2 in ocean exoplanets: Anovel CO_2 deposition mechanism. Astrophys J 2017;838:24.
[3] Wordsworth R, Kalugina Y, Lokshtanov S, Vigasin A, Ehlmann B, Head J, Sanders C, Wang H. Transient reducing greenhouse warming on early Mars. Geophys Res Lett 2017;44:665. doi:10.1002/2016GL071766.
[4] Wordsworth R. The climate of early Mars. Ann Rev Earth Planet Sci 2015;44:381–408.
[5] Gordon IE, Rothman LS, Hill C, Kochanov RV, Tan Y, Bernath PF. The HITRAN 2016 molecular spectroscopic database. J Quant Spectrosc Radiat Transf 2017;203:3–69.
[6] Tashkun SA, Perevalov VI, Gamache RR, Lamouroux J. CDSD-296, high-resolution carbon dioxide spectroscopic databank: an update. J Quant Spectrosc Radiat Transf 2019;228:124–31.
[7] Zak E, Tennyson J, Polyansky OL, Lodi L, Zobov NF, Tashkun SA, Perevalov VI. A room temperature CO_2line list with ab initio computed intensities. J Quant Spectrosc Radiat Transf 2016;177:31–42.
[8] Hashemi R, Gordon IE, Tran H, Kochanov RV, Karlovet EA, Tan Y, Lamouroux J, Ngo NH, Rothman RS. Revising the line-shape parameters for air- and self-broadened CO_2lines toward a sub-percent accuracy level. J Quant Spectrosc Radiat Transf 2020:107283.
[9] Baranov YI. Collision-induced absorption in the region of the ν_2+ $\nu_3$band of carbon dioxide. J Mol Spectrosc 2018;345:11–16.
[10] Asfin RE, Buldyreva JV, Sinyakova TN, Oparin DV, Filippov NN. Communication: evidence of stable van der waals CO_2 clusters relevant to venus atmosphere conditions. J Chem Phys 2015;142. 051101-4
[11] Oparin DV, Filippov NN, Grigoriev IM, Kouzov AP. Effect of stable and metastable dimers on collision-induced rototranslational spectra: carbon dioxide-rare gas mixtures. J Quant Spectrosc Radiat Transf 2017;196:87–93. doi:10.1016/j.jqsrt.2017.04.002.
[12] Oparin DV, Filippov NN, Grigoriev IM, Kouzov AP. Non-empirical calculations of rotovibrational band wings: carbon dioxide-rare gas mixtures. J Quant Spectrosc Radiat Transf 2020;247:106950–7. doi:10.1016/j.jqsrt.2020.106950.
[13] Shine KP, Ptashnik IV, Radel G. The water vapour continuum: brief history and recent developments. Surv Geophys 2012;33:535–55.
[14] Campargue A, Kassi S, Mondelain D, Vasilchenko S, Romanini D. Accurate laboratory determination of the near-infrared water vapor self-continuum: a test of the MTCKD model. J Geophys Res Atmos 2016;121:180–203.
[15] Serov EA, Balashov AA, Tretyakov MYu, Odintsova TA, Koshelev MA, Chistikov DN, et al. Continuum absorption of millimeter waves in nitrogen. J Quant Spectrosc Radiat Transf 2020;242:106774.
[16] Karman T, Miliordos E, Hunt KLC, Groenenboom GC, van der Avoird A. Quantum mechanical calculation of the collision-induced absorption spectra of N_2–$N_2$with anisotropic interactions. J Chem Phys 2015;142:084306.
[17] Gruszka M, Borysow A. Computer simulation of the far infrared collision induced absorption spectra of gaseous CO_2. Mol Phys 1998;93:1007–16.
[18] Vigasin AA. Water vapor continuum: whether collision-induced absorption is involved? J Quant Spectrosc Radiat Transf 2014;148:58–64.
[19] Frommhold L. Collision-induced absorption in gases. Cambridge University Press; 2006.
[20] Serov EA, Odintsova TA, Tretyakov MYu, Semenov VE. On the origin of the water vapor continuum absorption within rotational and fundamental vibrational bands. J Quant Spectrosc Radiat Transf 2017;193:1–12.
[21] Ptashnik IV, Klimeshina TE, Solodov AA, Vigasin AA. Spectral composition of the water vapour self-continuum absorption within 2.7 and 6.25 μm bands. J Quant Spectrosc Radiat Transf 2019;228:97–105.
[22] Tretyakov MYu, Koshelev MA, Serov EA, Parshin VV, Odintsova TA, Bubnov GM. Water dimer and the atmospheric continuum. Phys–Uspekhi 2014;57(11):1083–98.
[23] Odintsova TA, Tretyakov MYu, Zibarova AO, Pirali O, Roy P, Campargue A. Far-infrared self-continuum absorption of $H_2^{16}O$ and $H_2^{18}O$ (15-500 cm^{-1}). J Quant Spectrosc Radiat Transf 2019;227:190–200.
[24] Karman T, van der Avoird A, Groenenboom GC. Collision-induced absorption with exchange effects and anisotropic interactions: Theory and application to H_2–H_2. J Chem Phys 2015;142(8):084305.
[25] Hartmann JM, Boulet C, Jacquemart D. Molecular dynamics simulations for CO_2spectra. II. the far infrared collision-induced absorption band. J Chem Phys 2011;134(9):094316.
[26] Chistikov DN, Finenko AA, Lokshtanov SE, Petrov SV, Vigasin AA. Simulation of collision-induced absorption spectra based on classical trajectories and ab initio potential and induced dipole surfaces. I. Case study of N_2–N_2rototranslational band. J Chem Phys 2019;151:194106.
[27] Ho W, Birnbaum G, Rosenberg A. Far-infrared collision-induced absorption in CO_2 i. Temperature dependence. J Chem Phys 1971;55:1028–38.
[28] Bauer A, Godon M, Carlier J, Gamache RR. Absorption of a h_2o-CO_2mixture in the atmospheric window at 239GHz; h_2o-CO_2linewidths and continuum. J Mol Spectrosc 1996;176:45–57.
[29] Dagg IR, Reesor GE, Urbaniak JL. Collision induced microwave absorption in CO_2 and CO_2–Ar, CO_2−CH_4 Mixtures in the 2.3cm^{-1}Region. Can J Phys 1974;52:973–8.
[30] Frenkel L, Woods D. Microwave absorption in compressed CO_2. J Chem Phys 1966;44:2219.

[31] Dagg IR, Read LAA, Vanderkooy J. Far infrared laser system for the measurement of collision-induced absorption spectra. Rev Sci Instrum 1982;53:187–93.
[32] Occelli R, Blancher H, Bachet G, Coulon R. Difference-frequency source for very low optical frequencies spectroscopy: CO_2 induced spectra. Int J Infrared Millimeter Waves 1987;8:465–77.
[33] Dagg IR, Reesor GE, Wong M. A microwave cavity measurement of collision-induced absorption in $N_2$and CO_2 at 4.6 cm^{-1}. Can J Phys 1978;56:1037–45.
[34] Sullivan TE, Frenkel L. Microwave absorption in compressed CO_2 near 1.8 cm^{-1}. J Chem Phys 1970;52:3847–8.
[35] Ho W, Kaufman IA, Thaddeus P. Microwave absorption in compressed CO_2. J Chem Phys 1966;45:877–80.
[36] Maryott AA, Birnbaum G. Collision-induced microwave absorption in compressed gases i. dependence on density temperature, and frequency in CO_2. J Chem Phys 1962;36:2026–32.
[37] Dagg IR, Reesor GE, Urbaniak JL. Collision induced absorption in N_2,CO_2, and H_2at 2.3 cm^{-1}. Can J Phys 1975;53:1764–76.
[38] Birnbaum G, Ho W, Rosenberg A. Far-infrared collision-induced absorption in CO_2. II. pressure dependence in the gas phase and absorption in the Liquid. J Chem Phys 1971;55:1039–45.
[39] Kouroupetroglou GT, Boudouris G. Collision-induced absorption in CO_2at 0.091 cm^{-1}. J Phys Lett (France) 1981;42(19):441–3.
[40] Koshelev MA, Leonov II, Serov EA, Chernova AI, Balashov AA, Bubnov GM, Andriyanov AF, Shkaev AP, Parshin VV, Krupnov AF, Yu TM. New frontiers in modern resonator spectroscopy. IEEE Trans Terahertz Sci Technol 2018;8(6):773–83.
[41] Dymond JH, Marsh KN, Wilhoit RC, Wong KC. Virial coefficients of pure gases and mixtures. Virial coefficients of pure gases. Berlin Heidelberg New York: Springer-Verlag; 2002. p. 307.
[42] Dymond JH, Marsh KN, Wilhoit RC. Virial coefficients of pure gases and mixtures. Virial coefficients of mixtures. Berlin Heidelberg New York: Springer-Verlag; 2003. p. 369.
[43] Tretyakov MYu, Zibarova AO. On the problem of high-accuracy modeling of the dry air absorption spectrum in the millimeter wavelength range. J Quant Spectrosc Radiat Transf 2018;216:70–5.
[44] Liebe HJ, Layton DH. Millimeter-wave properties of the atmosphere: laboratory studies and propagation modeling. In: NTIA rep; 1987. p. 87–224.
[45] Koshelev MA, Serov EA, Parshin VV, Tretyakov MYu. Millimeter wave continuum absorption in moist nitrogen at temperatures 261–328 k. J Quant Spectrosc Radiat Transf 2011;112:2704–12.
[46] Podobedov VB, Plusquellic DF, Siegrist KE, Fraser GT, Ma Q, Tipping RH. New measurements of the water vapor continuum in the region from 0.3 to 2.7 THz. J Quant Spectrosc Radiat Transf 2008;109:458–67.
[47] Chistikov D.N. 2020. Private communication.
[48] Serov EA, Parshin VV, Bubnov GM. Reflectivity of metals in the millimeter wavelength range at cryogenic temperatures. IEEE Trans Microw Theory Tech 2016;64:3828–38.
[49] Bauer A, Godon M, Carlier J, Gamache RR. Continuum in the windows of the water vapor spectrum absorption of h_2o-ar at 239GHz and linewidth calculations. J Quant Spectrosc Radiat Transf 1998;59(3-5):273–85.
[50] Vigasin AA. On the temperature variations of the integrated absorption intensity in the oxygen fundamental. J Mol Spectrosc 2004;224(2):185–7.
[51] Buryak I, Frommhold L, Vigasin AA. Far-infrared collision-induced absorption in rare gas mixtures: quantum and semi-classical calculations. J Chem Phys 2014;140(15):154302.
[52] Chistikov D.N., Finenko A.A., Kalugina Y.N., Lokshtanov S.E., Petrov S.V., Vigasin A.A., Simulation of collision-induced absorption spectra based on classical trajectories and ab initio potential and induced dipole surfaces. II. Case study of CO_2–Ar rototranslational band. J Chem Phys; In Preparation.
[53] Hutson J, Ernesti A, Law MM, Roche CF, Wheatley RJ. The intermolecular potential energy surface for CO_2–Ar: fitting to high-resolution spectroscopy of van der waals complexes and second virial coefficients. J Chem Phys 1996;105:9130–40.
[54] Cui Y, Ran H, Xie D. A new potential energy surface and predicted infrared spectra of the ar-CO_2van der Waals complex. J Chem Phys 2009;130. 224311-7
[55] Dagg IR, Anderson A, Yan S, Smith W, Joslin CG, Read LAA. The quadrupole moment of cyanogen: a comparative study of collision-induced absorption in gaseous C_2N_2.CO_2 , and mixtures with argon. Can J Phys 1986;64(11):1475–81.
[56] Maryott AA, Kryder SJ. Collision-induced microwave absorption in Compressed Gases III. CO_2−Foreign -Gas Mixtures. J Chem Phys 1964;41:1580–2.
[57] Vigasin AA, Baranov YI, Chlenova GV. Temperature variations of the interaction induced absorption of CO_2 in the $\nu_1, 2\nu_2$region: FTIR measurements and dimer contribution. J Mol Spectrosc 2002;213(1):51–6.
[58] Vigasin AA. Bound, metastable and free states of bimolecular complexes. Infrared Phys 1991;32:461–70.
[59] Epifanov SY, Vigasin AA. Contribution of bound, metastable and free states of bimolecular complexes to collision-induced intensity of absorption. Chem Phys Lett 1994;225(4–6):537–41.
[60] Karman T, Gordon IE, van der Avoird A, Baranov YI, Boulet C, Drouin BJ. Update of the HITRAN collision-induced absorption section. Icarus 2019;328:160–75.
[61] FORTRAN. programs and data for CIA opacities of molecular complexes for planetary and stellar atmospheres. https://www.astro.ku.dk/~aborysow/programs/index.html.